ENGINEERING TRANSACTIONS • *Engng. Trans.* • **41**, 3–4, 351–360, 1993
Polish Academy of Sciences • Institute of Fundamental Technological Research

COMPARISON OF DAMAGE PROCESSES IN TWO AUSTENITIC STEELS UNDER THERMAL CYCLING AND CREEP CONDITIONS

L. KORUSIEWICZ, A. KRAJCZYK, Z. RECHUL
and R. ŻUCHOWSKI (WROCŁAW)

Processes of thermal cycling in materials are difficult to analyse beecause of complexity of the phenomena involved. The aim of the paper was to check the assumption that there is some similarity in failure mechanisms occurring under thermal cycling and stationary creep conditions. To this end deformation processes up to failure were analysed in various austenitic steels. The experiments were carried out on axially loaded cylindrical specimens made of austenitic steels. The specimens were tested in isothermal creep at temperatures 1173, 1123, 1073, 1023K and under thermal cycling conditions over the range 573 – 1173 K using three different thermal cycles: a saw-toothed and two trapezoidal ones. The investigation was aimed at assessing the contributions of creep and cyclic deformation to failure processes induced by various modes of thermal loading. The Monkman-Grant failure criterion was used to give a relationship between time to failure and steady deformation rate.

1. Introduction

Thermal fatigue is a process of progressive degradation of the material in machine parts or structures due to changes in internal energy induced by cyclic temperature changes [1].

It is generally acknowledged that thermal fatigue is caused by temperature changes and constraints imposed on thermal deformations, the constraints being due to either internal or external factors. A special case of thermal fatigue involves an element subject to a constant load under periodically changing temperature conditions and then it is termed "thermal cycling".

The service conditions inducing thermal fatigue are frequently encountered in power industry, steel and chemical plants. Other factors that promote material degradation under such conditions are oxidation, corrosion,

erosion or cavitation. It is generally accepted that no sound evaluation of the structural part condition is possible without taking account of thermal fatigue-related damage in such cases as those concerning heat exchangers, nuclear reactor components, internal combustion components, turbine blades and various tools for hot metal processing.

The acquired knowledge of the phenomenon [1–3] still does not allow safe and reliable procedures of design and life prediction to be established, though a large body of service-oriented theoretical material is available [4–10]. A natural trend of development will be a growing interest in complex stress cases; an example may be found in [11] where classical theories of creep have been used to model thermal fatigue processes under complex stress conditions. Thermal fatigue may be regarded as a result of superimposing processes of cyclic deformation which lead to growing amount of permanent plastic strain and creep [1], especially if high temperatures are involved. Simple superposition of the above processes, however, frequently fails to account satisfactorily for the phenomenon. Selection of a method for predicting life under thermal fatigue conditions is dependent upon the contributions of the two processes and therefore they must be assessed as precisely as possible. One way of estimating the contribution of cylic deformation and creep to the process of thermal fatigue has been presented in [11, 12], another method is put forward in this paper.

The present paper makes an attempt to give a description of processes occuring in two highly different austenitic steels under thermal cycling and isothermal creep conditions.

2. Materials

Two appreciably different grades of austenitic steel were used in the test: H23N18 and 50H17G17 of the following chemical compositions (wt%): 0.09C, 0.90Mn, 0.45Si, 25.1Cr, 17.6Ni, Fe – balance and 0.50C, 17.08Mn, 0.57Si, 16.2Cr, 0.22Ni, 0.072Al, 0.0014B, Fe – balance, respectively.

X-ray analysis revealed in both cases a microstructure of austenite plus carbides of the $M_{23}C_6$ type. The carbides had slightly different lattice parameters, for H23N18 steel $a_{Fe_\gamma} = 0.358_5$ nm and $a_{M_{23}C_6} = 1.070_5$ nm and for 50H17G17 steel $a_{Fe_\gamma} = 0.361_0$ nm and $a_{M_{23}C_6} = 1.061_3$ nm.

The average austenite grain diameter (d) was 50 μm, and the amount of the carbide phase was lower than 1% for H23N18 and $d = 4$ μm with the

carbide amount reaching 5% for the other material.

Appreciable differences were found in the linear coefficient of expansion. The average values over the temperature range $573 \rightarrow 1173K$ were $\alpha = 17.71 \times 10^{-6}\,[\mathrm{K}^{-1}]$ for H23N18 and $\alpha = 22.04 \times 10^{-6}\,[\mathrm{K}^{-1}]$ for 50H17G17. Mechanical properties of the two steels also differed appreciably (Table 1).

Table 1. Mechanical properties of H23N18 and 50H17G17 steels.

Material	R_m [MPa]	$R_{0.2}$ [MPa]	A_{10} [%]	Z_0 [%]	HV	$R_m/R_{0.2}$
H23N18	578	226	49	60	161	2.6
50H17G17	1122	804	17	19	337	1.4

R_m – ultimate tensile strength, $R_{0.2}$ – yield point (0.2% offset), A_{10} – elongation, Z_0 – cross-section area reduction, HV – Vickers hardness.

3. Experiments and results

The main body of experiments were carried out under isothermal creep conditions at four temperatures: 1023, 1073, 1123 and 1173 K and under ($573 \leftrightarrow 1173$ K) – temperature cycling conditions using three different thermal cycles (Fig. 1):

- a saw-toothed cycle (in what follows denoted as S);
- a trapezoidal cycle with the maximum temperature holding time equal to 30 s (denoted T30);
- a trapezoidal cycle with the maximum temperature holding time equal to 120 s (denoted T120).

The specimens were loaded with a constant force resulting in the initial stress $\sigma_0 = 60$ MPa and then were alternately resistance-heated and air-cooled. The heating-up rate was held constant [10K/s]. Temperature changes were recorded using a PtRh-Pt thermocouple welded midway between the specimen ends, and elongation signals were picked up with a LVDT. The following characteristics were determined: the number of cycles to failure (N_f) and the corresponding time (t_f), steady creep and deformation rate (V_s), percent elongation over a tenfold gauge length (A_{10}) and actual rupture deformation (φ). The elongation under cycling conditions was measured at the minimum temperature of the cycle. Average values of the above characteristics are listed in Table 2.

Table 2. Average values of the results obtained from creep and thermal cycling experiments on H23N18 and 50H17G17 steels.

Loading mode	Temperature T [K]	Number of cycles to failure N_f	Time to failure t_f [s]	Steady-state deformation rate V_s [s^{-1}]	Elongation A_{10} [%]	Actual rupture elongation φ [%]	Accelerated deformation rate proportion [%]	Material
creep	1173	–	3148	5.26×10^{-5}	22.7	1.02	30	H23N18
	1123	–	13672	1.09×10^{-5}	21.3	1.06	30	
	1073	–	95614	1.44×10^{-6}	18.3	0.75	21	
	1023	–	545775	1.70×10^{-7}	18.5	0.43	26	
creep	1173	–	533	3.25×10^{-4}	24.7	1.66	36	50H17G17
	1123	–	1930	7.31×10^{-5}	21.4	1.46	54	
	1073	–	8503	1.75×10^{-5}	21.3	1.45	44	
	1023	–	66865	1.70×10^{-6}	19.0	1.48	37	
T120	573 ⇔ 1173	25	6318	2.28×10^{-5}	21.1	0.93	33	H23N18
T30		32	5118	2.28×10^{-5}	22.5	0.97	35	
S		160	22567	3.97×10^{-6}	18.5	0.85	59	
T120	573 ⇔ 1173	5	1028	1.20×10^{-4}	20.7	1.44	41	50H17G17
T30		11	1610	6.98×10^{-5}	19.9	1.47	46	
S		73	7901	1.22×10^{-5}	16.7	1.32	33	

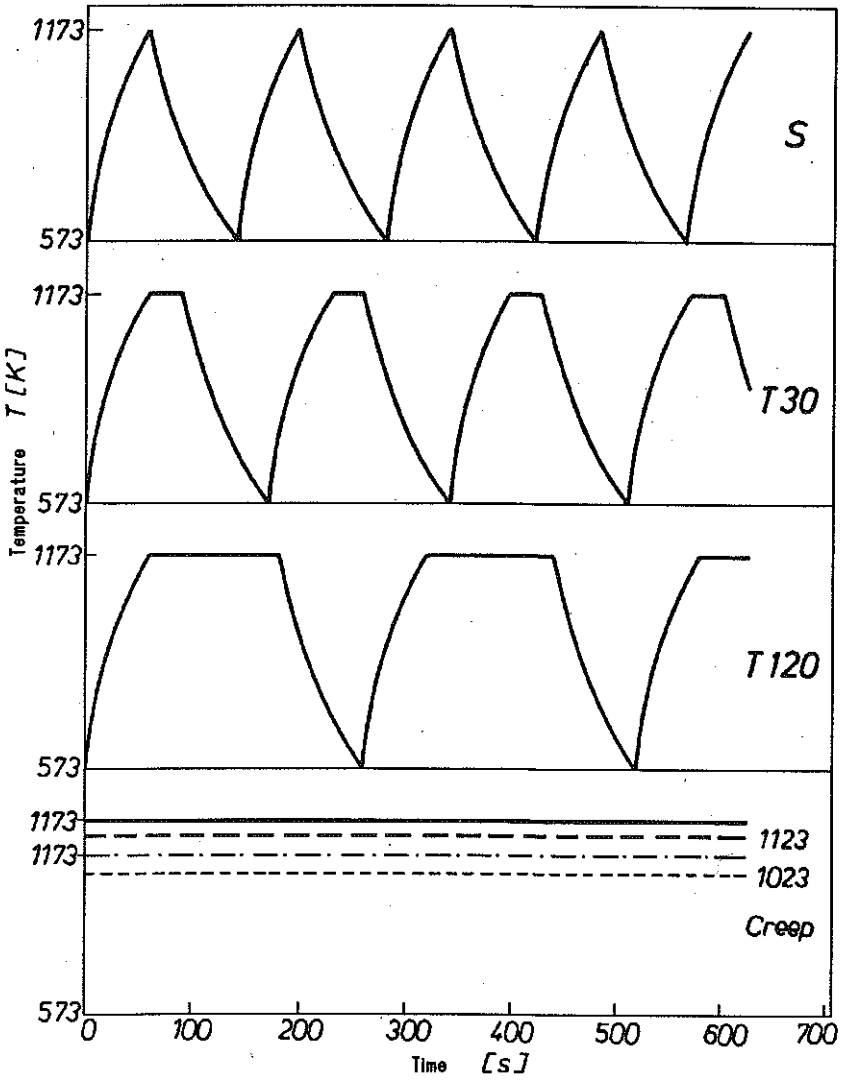

FIG. 1. Thermal loading modes used in the investigations: S – saw-toothed cycle, T30 – trapezoidal cycle with the maximum temperature holding time equal to 30 s, T120 – trapezoidal cycle with the maximum holding time equal to 120 s, creep – isothermal creep.

4. ANALYSIS OF THE RESULTS

The effect of a loading mode on the life of specimens made of one of the two materials was evaluated by using the Monkman-Grant relationship [6] in which the separation of the material was assumed as the failure

criterion. The Monkman–Grant relationship expresses time to fracture t_f as a function of steady deformation rate V_s

$$t_f = CV_s^{-m} \tag{1}$$

and is shown graphically in Fig. 2. The constants in Eq. (1) were determined from the present experiments. Statistical analysis showed that for 50H17G17 specimens for all the loading modes used, the constants in Eq. (1) were the same (line *3* in Fig. 2).

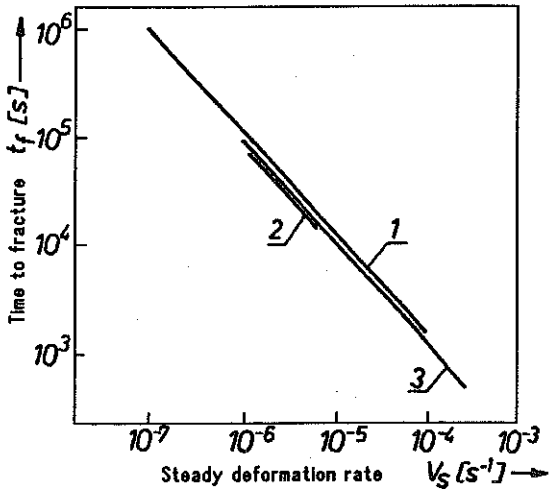

FIG. 2. Relationship between time to fracture (t_f) and steady deformation rate (V_s) at 60 MPa: *1* – H23N18 – creep, T30 and T120; *2* – H23N18 – S; *3* – 50H17G17 – creep, S, T30 and T120.

The H23N18 specimens gave different constants for different loading modes. The obtained values of constants in Eq. (1) are given in Table 3.

Table 3. Constants of the Monkman – Grant equation with linear correlation probabilities.

Loading modes	Constants		Number of specimens	Linear correlation probability	Material
	C	m			
Creep T30 T120	0.30	0.93	25	0.999	H23N18
S	0.20	0.93	9	0.999	
Creep T120 T30 S	0.23	0.93	40	0.999	50H17G17

5. Metallographic examination

The metallographic examination was carried out on the longitudinal sections as well as on fracture surfaces of failed specimens using light microscopy, TEM and SEM. The microscopic examination showed that in 50H17G17 specimens for all the loading modes used the grain size remained constant and equal to $3 \div 5\,\mu m$. It was probably due to a hindering effect of the finely dispersed carbide phase whose amount in this steel was found to reach 5%.

Another pattern of behaviour was found in H23N18 steel where the carbide phase content did not exceed 1%. The grain size in creep specimens was found to be an increasing linear function of temperature, starting from $d = 50\,\mu m$ for the virgin material and reaching $200\,\mu m$ for the highest temperature of creep tests (1173 K). By contrast, no substantial effect of the cycle type on the grain size was detected in thermally cycled specimens. The determined grain size value was $130 \div 160\,\mu m$ and could be compared with that found in creep specimens in the 1023 – 1123 K range.

The thin foil examination revealed the presence of subgrains in both steels. In 50H17G17 steel the subgrain boundaries were of a mixed type (polygonal + cellular) and the subgrain interior showed a high density of dislocations and stacking faults. In H23N18 steel tested in creep and (T30, T120) – cycling the subgrain boundaries were mainly of the cellular type and the dislocation density was generally high. By contrast, the S-cycled specimens had an entirely different dislocation structure. The subgrain boundaries were chiefly of the polygonal type and the dislocation density was low.

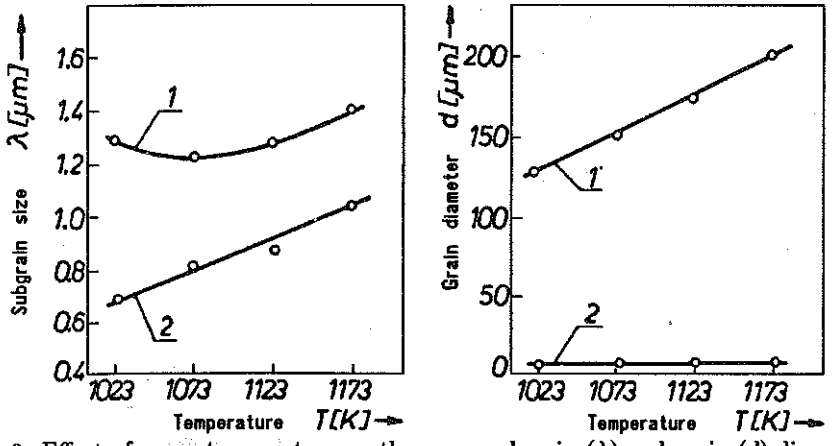

FIG. 3. Effect of creep temperature on the mean subgrain (λ) and grain (d) diameter: *1* – H23N18, *2* – 50H17G17.

In both steels in creep specimens the subgrain size was found to rise with temperature. The effect of creep temperature on the grain and subgrain size is presented in Fig. 3. In all H23N18 specimens that underwent thermal cycling, regardless of the cycle shape: S, T30 or T120, the prevailing crack form was a wedge one (Fig. 4). Similar behaviour was found in creep

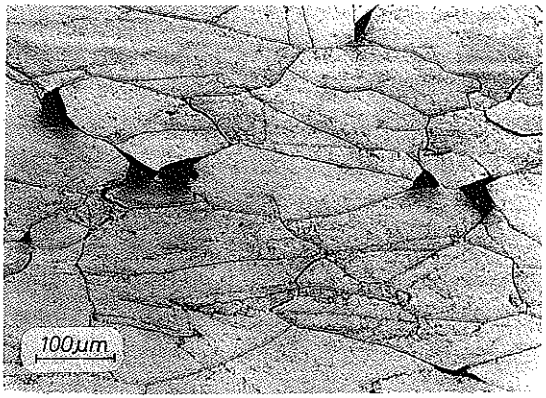

FIG. 4. Wedge-like cracks H23N18; T30.

specimens from the 1073 – 1173 K range, the crack size being smaller with the test temperature decreasing. In H23N18 specimens subjected to creep at the lowest temperature used (1023 K), the cracks were of a mixed (wedge + void) type. These specimens were the only ones found to lack the zone of deformed grains in the vicinity of the fracture surface. As regards the other steel, in all cases the prevailing form of a crack was a wedge one and the cracks were mainly originated as the matrix – carbide interface. Those

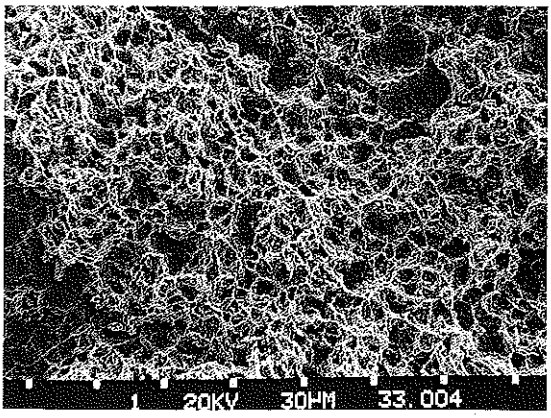

FIG. 5. Transgranular ductile fracture 50H17G17 – creep, 1023 K.

cracks were then observed to grow and finally to create a fine network in the neighbourhood of the rupture surface. Fractographic examination of 50H17G17 steel revealed in all cases of loading the transgranular ductile fracture (Fig. 5), while in H23N18 material the fracture paths observed were both through and along the grain boundaries. In the latter case the percentage of intergranular fracture was higher as the creep temperature was lowered, and at a temperature of 1023 K it exceeded 90% (Fig. 6).

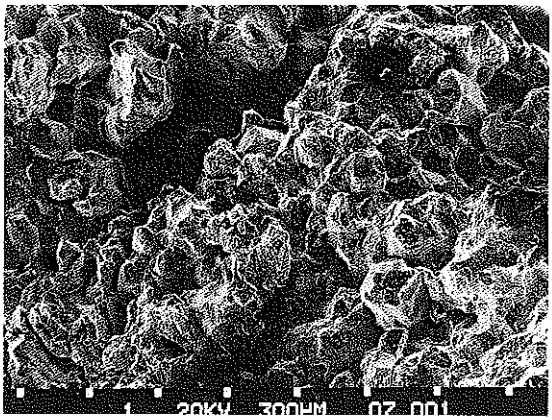

FIG. 6. Intergranular fracture 50H17G17 – creep, 1023 K.

6. SUMMARY OF THE RESULTS

The experiments enabled the authors to detect many significant differences between the two steels which cast some light on the interrelation between isothermal creep and thermal cycling.

1. The damage accumulation process in 50H17G17 is governed by the same equation for two principal modes of loading while in H23N18 the equation coefficients valid for creep differ from those for thermal cycling.

2. The life of H23N18 specimens is longer than that for the other steel, the difference being the largest for creep and the smallest for thermal cycling with a cycle of zero holding time (cycle S).

3. The observed differences in time to failure result from the corresponding differences in the steady deformation (creep) state.

4. Percent elongation under creep conditions is higher in 50H17G17 while for the other mode of loading H23N18 material exhibits larger values.

5. Proportion of the 3rd (accelerated) stage of deformation is higher in 50H17G17 tested in creep and in thermal cycling of the T30 and T120 type.

For cycle S the higher proportion of the 3rd stage is observed in H23N18.

6. 50H17G17, in contrast to the other material, shows no signs of grain growth and fracture is of transgranular (ductile) type.

REFERENCES

1. R.ŻUCHOWSKI, *Analysis of failure process under conditions of thermal fatigue* [in Polish], Technical University of Wrocław, Wrocław 1986.
2. A.WERÓŃSKI, *Thermal fatigue of metals*, WNT, Warszawa 1983.
3. Z.ORŁOŚ, *Thermal cycling*, Wyd. Nauk. PWN, Warszawa 1991.
4. R.ŻUCHOWSKI, N.BUBA, *Assessment of durability under conditions of thermal cycling on the basis of the results obtained in creep*, Res Mechanica, **5**, 4, 317–322, 1982.
5. R.ŻUCHOWSKI, *Specific strain work as both a failure criterion and material damage measure*, Res Mechanica, **27**, 4, 309–322, 1989.
6. F.C.MONKMAN, N.J.GRANT, *An empirical relationship between rupture life and minimum creep rate in creep-rupture test*, ASTM Preprint 72, Annual Meeting, June 17, 1956.
7. R.ŻUCHOWSKI, L.KORUSIEWICZ, *Acoustic emission as a measure of material damage under thermal cycling*, J.Acoustic Emission, **2**, 4, 272–274, 1983.
8. C.DEGALLAIX, C.KORN, G.PLUVINAGE, *Lifetime prediction on* Cr-Mo-V *and* 316L *steels under thermal and mechanical cycling*, Fatigue and Fracture of Engng. Materials and Structures, **13**, 5, 473–485, 1990.
9. D.A.BOISMIER, H.SEHITOGLU, *Thermo-mechanical fatigue of* MAR-M247. *Part 1. Experiments*, Trans. ASME J. Engng. Materials and Technology, **112**, 1, 68–79, 1990.
10. H.SEHITOGLU, D.A.BOISMIER, *Thermo-mechanical fatigue of* MAR-M247. *Part 2. Life prediction*, Trans. ASME J. Engng. Materials and Technology, **112**, 1, 80–89, 1990.
11. R.ŻUCHOWSKI, *Effect of stress state type on deformation process of austenitic steel under thermal cycling conditions*, Intern. J. Pressure Vessels and Piping, **46**, 279–288, 1991.
12. G.R.HALFORD, S.S.MANSON, *Life prediction of thermal-fatigue using strain range partitioning*, Thermal Fatigue of Materials and Components, ASTM STP 612, 239–254, 1976.

INSTITUTE OF MATERIAL SCIENCE AND APPLIED MECHANICS
WROCŁAW UNIVERSITY OF TECHNOLOGY, WROCŁAW.

Received July 14, 1993.